

PAPER • OPEN ACCESS

Development of a Physics-Based Dynamic Model For a Micro Gas Turbine Engine

To cite this article: Ibrahim M.A Ibrahim 2025 *J. Phys.: Conf. Ser.* **3070** 012016

View the [article online](#) for updates and enhancements.



UNITED THROUGH SCIENCE & TECHNOLOGY

 **The Electrochemical Society**
Advancing solid state & electrochemical science & technology

**248th
ECS Meeting**
Chicago, IL
October 12-16, 2025
Hilton Chicago

*Science +
Technology +
YOU!*

**Register by
September 22
to save \$\$**

REGISTER NOW

The banner features a woman in a brown blazer smiling and gesturing, set against a blue background with a molecular structure pattern. The top and bottom of the banner are decorated with a repeating circular logo.

Development of a Physics-Based Dynamic Model For a Micro Gas Turbine Engine

Ibrahim M.A Ibrahim^{1*}

¹Department of Aircraft Mechanical Engineering, Military Technical College, Cairo, Egypt

*E-mail: ibrahimateya@mtc.edu.eg

Abstract. This paper presents a physics-based, detailed nonlinear dynamic mathematical model (MTCturb) of a micro SR-30 gas turbine engine (GTE) using a component matching method. The model integrates individual component of the gas turbine engine capturing thermodynamic and aerodynamic interactions through nonlinear dynamic equations. MTCturb is designed to predict the engine shaft speed (RPM) response with fuel flow as the primary input, accurately simulating both transient and steady-state performance under varying operating conditions. The model is validated against experimental data and high-fidelity simulation results from GasTurb 10, demonstrating strong agreement and confirming its accuracy and predictive capability. Additionally, a graphical user interface (GUI) is developed in MATLAB to enhance model accessibility, enabling users to interactively visualize simulations, adjust input parameters, and analyze system responses. This work provides a valuable tool for control design, optimization, and further research on gas turbine dynamics.

1. Introduction

Micro gas turbine engines (MGTEs) are commonly employed in unmanned aerial vehicles. Moreover, they serve as valuable academic test benches for education and research, offering a hands-on platform for exploring thermodynamic principles, propulsion mechanisms, and advanced control methodologies. Their small size, high power-to-weight ratio, and straightforward operation make them well-suited for experimental studies across various disciplines, including aerospace engineering, energy systems, and control applications. However, MGTEs often suffer from reduced operational lifespan due to high thermal and mechanical stresses, requiring accurate modeling to enhance durability and reliability through optimized materials and cooling strategies. The typical maximum operational lifetime of an MGTE is around **25** hours, making it important to develop accurate physics-based models to extend operational efficiency and reduce the need for extensive experimental research. Furthermore, this model serves as a valuable tool for developing, testing, and fine-tuning control systems for gas turbine engines. It also enables the simulation of critical transient scenarios that would be too risky to replicate on the actual engine due to the potential for damage.

Gas turbine engine (GTE) modeling approaches are generally classified into two main categories: physics-based modeling (also known as white-box modeling) and data-driven modeling methods [1]. Data-driven modeling, often referred to as black-box modeling, is particularly useful when little or no information is available about the system's underlying physics. This approach constructs models based on observed data rather than relying solely on first-principles equations, emphasizing the identification of relationships between system variables through operational input and output data. One of the most widely used techniques in data-driven modeling is the artificial neural network (ANN), which is inspired



by the structure and functionality of the human brain [2]. ANN-based modeling has been extensively applied in gas turbine engine simulations by various researchers [3–5]. However, a key challenge in using ANN is its limited ability to provide accurate predictions when operating outside the data range on which it was trained. Additionally, gas turbine engines function under non-stationary conditions, leading to potential unseen operational scenarios in the collected data. This increases the complexity of the modeling process, as the neural network must be trained on a sufficiently large dataset covering all possible operating conditions. Consequently, this requirement extends training time and increases the risk of network overfitting [4].

Physics-based models rely on first-principles equations and are applicable when sufficient information about the system's physics is available [6]. This approach has been extensively employed over the years to model gas turbine engines across their entire operating range and under various operation conditions. A physics-based gas turbine model typically consists of two key performance models: the off-design steady-state model and the off-design transient model. The engine is considered to be in a steady-state condition when its internal parameters reach thermodynamic equilibrium. However, unlike steady-state models, which only determine the final performance outcomes, transient models account for the dynamic response of the engine as it transitions between states due to changes in power demand, fuel flow, or ambient conditions [7].

In off-design steady-state analysis, all engine components must satisfy mass, momentum, energy, and work balance conditions while aligning with performance maps to ensure a consistent operating state. This process, known as component matching, relies on iterative numerical methods to determine the correct operating point. Two widely used iteration techniques for achieving component matching are the serial nested loops method and the matrix method [8]. Both approaches iteratively adjust variables (guesses) until specific constraints, such as mass flow and work balance, are met. The serial nested loops method is relatively straightforward to implement, making it suitable for personal computer programs. However, its computational efficiency declines significantly when the number of nested loops exceeds five [8–10]. Conversely, the matrix method reformulates the matching equations as a system of nonlinear algebraic equations, which are then solved using numerical techniques like the Newton-Raphson method. This approach is faster and more efficient, particularly for complex engine models, making it the preferred technique for gas turbine engine simulations [11, 12].

In off-design transient calculations, gas turbine engines (GTEs) exhibit three primary types of dynamics that must be considered during dynamic modeling: shaft dynamics, pressure dynamics, and temperature dynamics [13]. During transient conditions, such as acceleration, deceleration, or load changes, flow and work imbalances occur. To address these imbalances, two key modeling approaches are commonly used: the Constant Mass Flow (CMF) method [14, 15], and the Inter-Component Volume (ICV) method [16].

The CMF method focuses exclusively on shaft dynamics, assuming that the mass flow entering a component must equal the mass flow exiting it at each iteration step while solving transient equations [17]. In contrast, the ICV method is a widely adopted approach for capturing the dynamic behavior of GTEs. It accounts for the time-dependent variations in pressure, temperature, and mass flow across different engine components by introducing control volumes between them and applying conservation laws for mass and energy [18]. The transient behavior of GTEs is governed by differential equations that describe the evolution of key state variables, including rotational speed, pressure, and temperature, over time. These equations are typically solved using numerical integration techniques, such as the Euler method [19], and Runge-Kutta methods [16], to ensure accurate transient performance predictions.

Several studies have been conducted to evaluate and optimize the performance of micro gas turbine engines (MGTEs) under off-design conditions. Singh et al. [20] developed a mathematical model based on the state variable method to simulate both off-steady-state and transient performance of the SR-30 MGTE. Nott et al. [21] explored the application of artificial intelligence techniques for health monitoring and sensor validation in micro turbine engines. Lichtsinder et al. [22] proposed a quasi-linear modeling approach for micro turbine engines, aimed at facilitating controller design. Additionally, Valencia et al. [23] developed a physics-based model of the SR-30 MGTE using MATLAB/Simulink.

This paper presents the development of a detailed nonlinear physics-based model for the SR-30 micro gas turbine engine. The model is designed to predict the engine's off-design steady-state and transient behavior across its full operating range. The proposed approach is systematically implemented through the development of a simulator featuring a graphical user interface (GUI) in the MATLAB environment. For the off-design steady-state model, the Newton-Raphson method is employed to solve nonlinear algebraic equations. In transient performance analysis, the Constant Mass Flow (CMF) method is used to represent shaft dynamics, while the Euler integration method is applied to compute the surplus torque resulting from the work imbalance between the compressor and turbine. The accuracy of the model is

validated by comparing its steady-state and transient simulation results with experimental data from SR-30 engine tests and results from GasTurb10 high-fidelity simulation software.

The rest of this paper is organized as follows: Section two outlines the specifications of the SR-30 micro gas turbine (MGT) engine used in this study. Section three provides a detailed explanation of the methodology for developing the physics-based model. Section four presents and discusses the results obtained from this study, while Section five summarizes the conclusion.

2. Micro gas turbine engine

Micro gas turbine engines (MGTEs) are becoming increasingly popular in many industrial and aerospace applications due to their high power-to-weight ratio, multi-fuel capability, and simple design. In this study, the Turbine Technologies SR-30 MGTE, shown in Figure 1, is modeled. The engine operates by drawing ambient air through a bell-shaped intake, which is then compressed by a single stage radial flow compressor, increasing its pressure and temperature. The compressed air then enters a reverse flow annular combustion chamber, where fuel delivered through six high-pressure atomizing nozzles is mixed with the compressed air and ignited. The high energy combustion gases are directed into a single stage axial flow turbine, which extracts energy to drive the compressor. The remaining gases are then expelled through a convergent exhaust nozzle, where their thermal energy is converted into kinetic energy in the form of thrust.



Figure 1. SR-30 micro gas turbine engine.
Taken from [3]

3. Physics-based detailed nonlinear dynamic model

Before initiating the modeling process, several assumptions are made:

1. Thermo-physical properties such as the gas constant (γ), specific heat capacity (C_p), lower heating value of the fuel (LHV), and universal gas constant (R) are considered constant.
2. The compression and expansion processes are assumed to be isentropic.
3. The thermal inertia of engine components is neglected.
4. The combustion chamber pressure loss is considered constant
5. , No bleed air is accounted for in the model.

Figure 2 shows a sketch of SR-30 MGT engine with its stations numbers.

3.1 Inlet

It ensures that the airflow enters the compressor with minimal turbulence and uniform distribution. The total temperature and pressure at the inlet component exit are calculated as shown in the following equations,

$$T_{0a} = T_a * (1 + \frac{\gamma_a - 1}{2} * M^2) \quad (1)$$

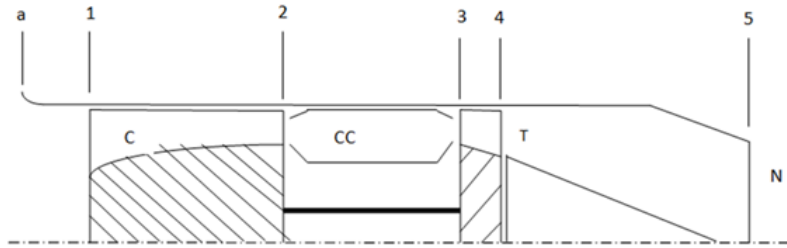


Figure 2. Notation and station numbering for SR-30 MGT engine.

$$T_{0a} = T_{01} \quad (2)$$

$$P_{01} = (1 - \Delta PR_{in}) * P_{0a} \quad (3)$$

where, M is the mach number, T_0 is the the stagnation temperature, T is the static temperature, P_0 is the the stagnation pressure, and ΔPR_{in} is the inlet pressure losses.

3.2 Compressor

The main role of a compressor is to raise the total pressure of the incoming air. Its performance is typically depicted using a compressor map, which presents a major challenge in constructing a physics-based nonlinear dynamic model. To overcome this challenge, a map scaling technique can be utilized to adapt an existing published component map to create a new compressor map [24]. Compressor maps should be digitized and incorporated into the simulation program using look-up tables, which offer a flexible and efficient way to represent component performance. Once the required compressor map is generated, the compressor characteristics can be expressed as functions of relative speed $\%N_C$ and beta value β , as illustrated in the following equations.

$$\pi_C = fn(\beta_C, \%N_C) \quad (4)$$

$$\left(\frac{m^{\bullet} \sqrt{\theta}}{\delta} \right)_C = fn(\beta_C, \%N_C) \quad (5)$$

$$\eta_C = fn(\beta_C, \%N_C) \quad (6)$$

where,

$$\theta = \frac{T_{01}}{288.15} \quad (7)$$

$$\delta = \frac{P_{01}}{101325} \quad (8)$$

where, $\left(\frac{m^{\bullet} \sqrt{\theta}}{\delta} \right)$ is the corrected mass flow rate.

Once the compressor characteristics are determined, the exit conditions of the compressor can be computed using the following equations:

$$P_{02} = \pi_C * P_{01} \quad (9)$$

$$T_{02} = T_{01} * \left[1 + \frac{\pi_C^{\left(\frac{\gamma_a - 1}{\gamma_a} \right)} - 1}{\eta_C} \right] \quad (10)$$

$$m_2^{\bullet} = \left(\frac{m^{\bullet} \sqrt{\theta}}{\delta} \right)_C * \frac{\delta}{\sqrt{\theta}} \quad (11)$$

$$W_c^{\bullet} = m_1^{\bullet} * c_{pa} * (T_{02} - T_{01}) \quad (12)$$

where, W_c^{\bullet} is the compressor power, m^{\bullet} is the mass flow rate, η_C is the compressor isentropic efficiency, and π_C is the compressor total pressure ratio.

3.3 Combustor

The primary function of the combustor is to enhance the potential energy of the air by burning a mixture of fuel and compressed air. The exit parameters of the combustor can be determined based on the inlet conditions, fuel flow rate W_F , combustion efficiency η_{CC} , and total pressure loss within the combustor ΔPR_{CC} , as shown in the following equations:

$$m_3^\bullet = m_1^\bullet + WF \quad (13)$$

$$T_{03} = \frac{m_3^\bullet * c_{p_a} * T_{02} + WF * LHV * \eta_{CC}}{m_3^\bullet * c_{p_g}} \quad (14)$$

$$P_{03} = P_{02} * (1 - \Delta PR_{CC}) \quad (15)$$

where, LHV is the fuel lower heating value

3.4 Turbine

The turbine's primary function is to extract energy from the high-temperature gases generated in the combustor, supplying power to the compressor and other auxiliary systems. Similar to compressors, determining the turbine exit conditions requires knowledge of the turbine inlet conditions and its key characteristics given by turbine map, including mass flow rate, pressure ratio, and isentropic efficiency, for a given spool speed and beta line value. Once the scaled turbine map is established, the turbine exit conditions can be computed using the following equations:

$$P_{04} = \frac{P_{03}}{\pi_T} \quad (16)$$

$$T_{04} = T_{03} * \left[1 - \eta_T (1 - \pi_T^{\frac{\gamma_g - 1}{\gamma_g}}) \right] \quad (17)$$

$$W_T^\bullet = m_3^\bullet * c_{p_g} * (T_{03} - T_{04}) \quad (18)$$

where, W_T^\bullet is the turbine power, η_T is the turbine isentropic efficiency, and π_T is the turbine total pressure ratio.

3.5 Exhaust nozzle

The primary function of the exhaust nozzle is to accelerate the exhaust gases exiting the turbine to produce thrust. It achieves this by converting the remaining thermal and pressure energy of the exhaust gases into kinetic energy, increasing the velocity of the airflow as it exits the engine. Two possible flow conditions can occur in the exhaust nozzle:

1. If the static pressure P_5 is greater than the critical pressure, the flow remains unchoked, meaning the Mach number at the nozzle exit $(M_5) < 1$.
2. If the static pressure P_5 is equal to or lower than the critical pressure, the flow becomes choked, resulting in a Mach number of $(M_5) = 1$

The exhaust nozzle output parameters can be calculated as shown in the following equations,

$$T_{05} = T_{04} \quad (19)$$

$$P_{05} = (1 - \Delta PR_{ex}) * P_{04} \quad (20)$$

where, ΔP_{ex} is the exit nozzle pressure losses.

3.6 Rotor dynamics

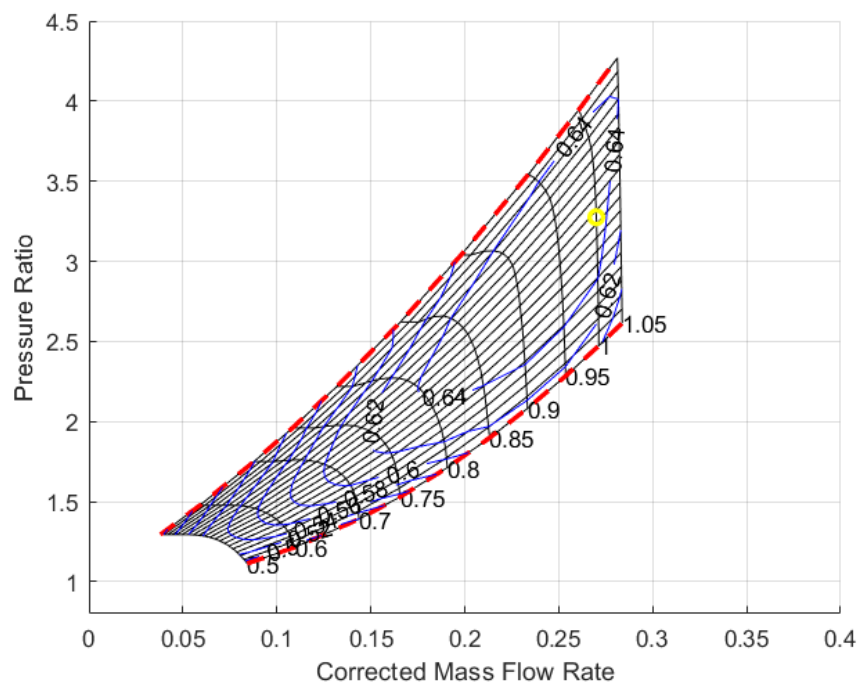
According to Newton's second law for rotational motion, the shaft dynamics of the SR-30 MGT engine are governed by the balance between the torque produced by the turbine and the torque required by the compressor. This relationship is mathematically expressed as follows:

$$\frac{dN}{dt} = \frac{3600}{4 * \pi^2 * N * J} [W_T^\bullet - W_c^\bullet] \quad (21)$$

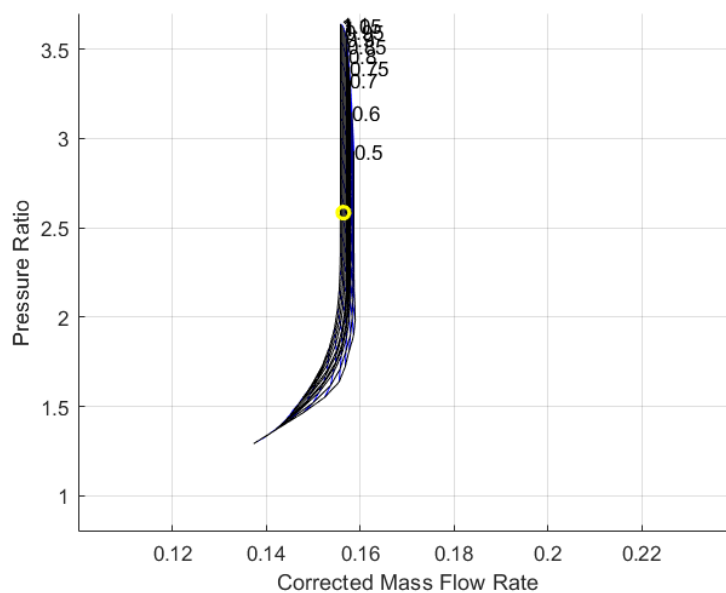
where, J is the shaft polar moment of inertia.

3.7 Off design steady state performance

Published compressor and turbine maps available in [25] have been used for off-design simulations using a simple scaling method [24]. Figure 4 illustrates the scaled compressor and turbine maps used in the development of the physics based model of the SR-30 MGT engine.



(a) Scaled compressor map.



(b) Scaled turbine map.

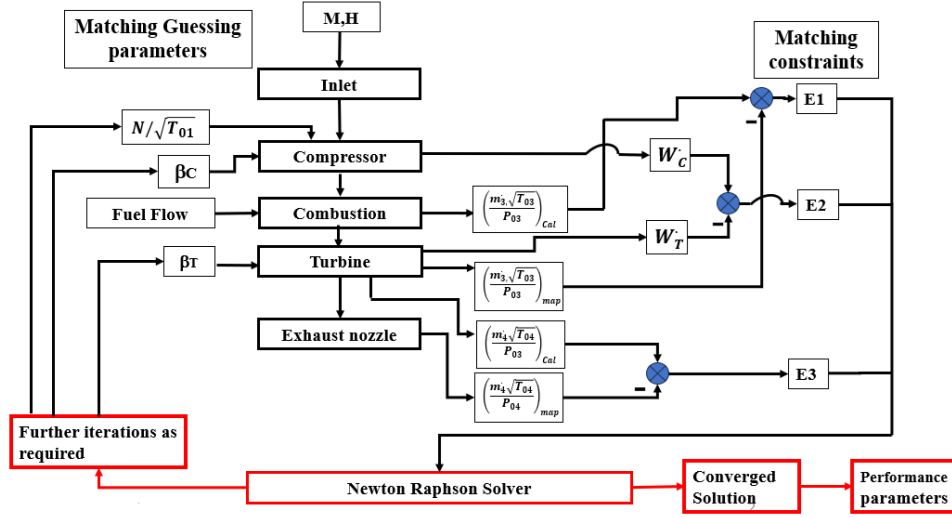
Figure 3. The SR-30 MGT engine scaled compressor and turbine map.

The system of nonlinear thermodynamic algebraic equations (1 to 20), which describe the steady-state performance of the engine, is solved iteratively using the Newton-Raphson method. This ensures proper

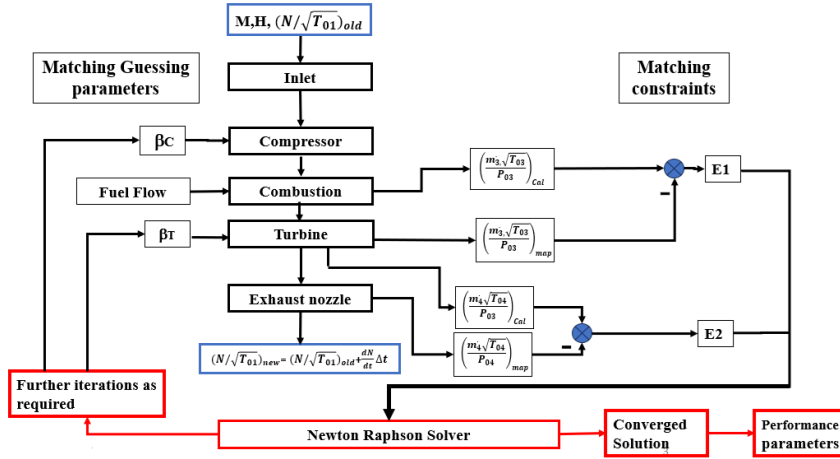
matching between all engine components. For a single-spool turbojet engine, the three matching variables (β_c, β_T, N) and the three corresponding matching constraints (E_1, E_2, E_3) are defined as follows:

$$E_1 = \frac{m_T^* - m_C^*}{m_C^*}, E_2 = \frac{m_n^* - m_T^*}{m_T^*}, E_3 = \frac{W_T^* - W_C^*}{W_C^*} \quad (22)$$

During iteration the matching guesses are continually updated until the matching constraints are satisfied as shown in Figure 4a.



(a) Off-design steady-state.



(b) Off design transient.

Figure 4. Off-design performance component matching.

3.8 Off design transient performance

In this study, the Constant Mass Flow (CMF) method is employed to model the shaft dynamics of the SR-30 MGTE [13]. Additionally, the Euler integration method (Eqn(23)) is used to integrate the excess torque generated by the difference in work between the compressor and the turbine (Eqn(21)). To simulate the engine's transient behavior, the calculation process follows the steps illustrated in Figure 4b.

$$N_{new} = N_{old} + \frac{dN}{dt} * \Delta t \quad (23)$$

To improve convergence efficiency and minimize computation time, two methods are implemented. First, the guessing parameters are initialized either using the last successfully converged point or a

predefined starting point based on the fuel flow. Second, if the sum of squared errors increases compared to the previous iteration, the Bisection method is applied. This method searches for an optimal variable value in the predicted direction to enhance convergence and find a more accurate solution.

4. Results and Discussion

A MATLAB-based simulator with a graphical user interface (GUI) has been developed, as illustrated in Figure 5. The MTCturb simulator facilitates the visualization and analysis of gas turbine engine performance across various operating conditions. It serves as a valuable tool for research, education, and gas turbine performance assessment.

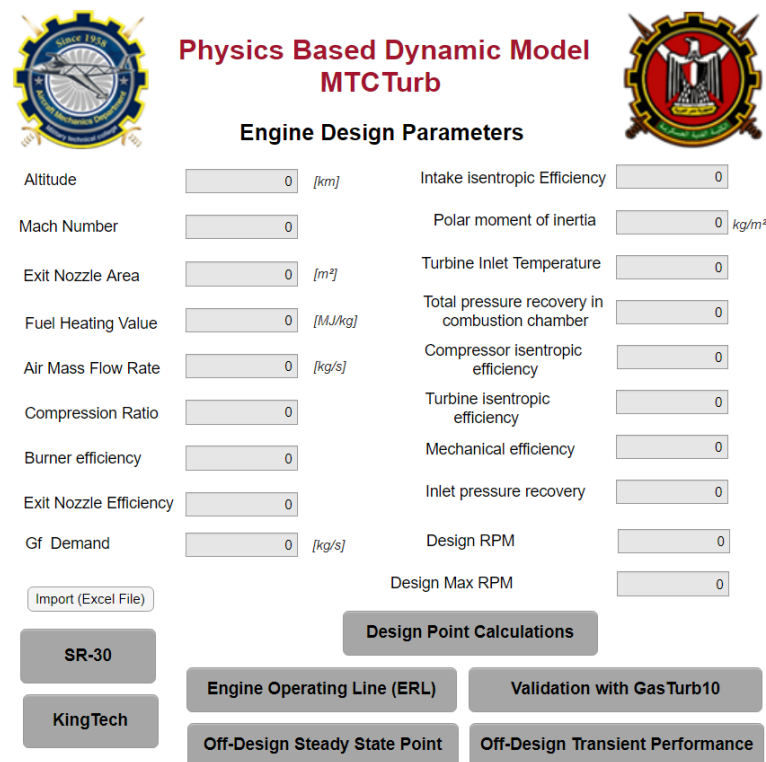


Figure 5. Physics Based Dynamic Model MTCturb.

To build confidence in the developed physics based dynamic model, its performance simulations are validated against experimental data from testing of the SR-30 MGTE, as well as simulation results from the high-fidelity GasTurb10 software [26]. The validation process is conducted in three stages: first, design point validation; second, off-design steady-state validation; and third, off-design transient validation.

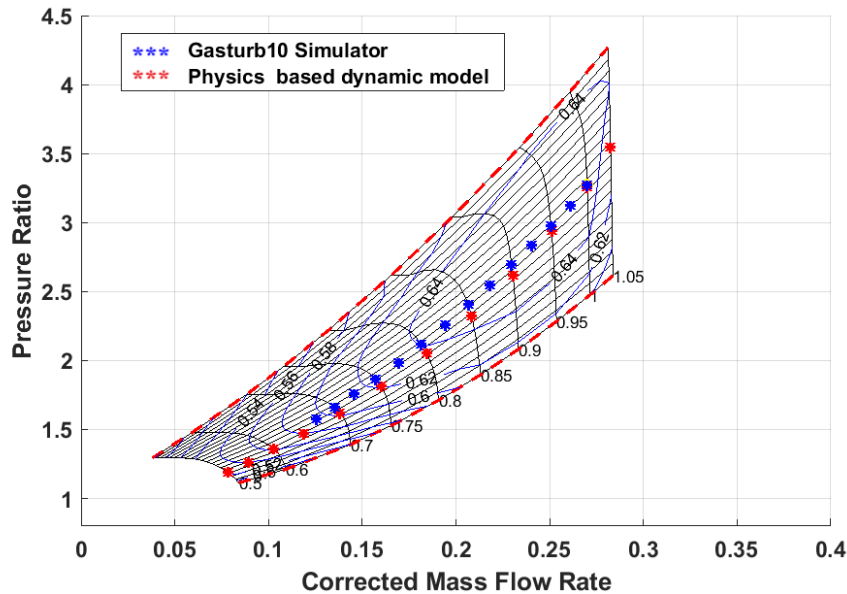
Firstly, The MTCturb model was run at design point condition at SLS (Altitude= 0 m), Mach number ($Mo=0$), shaft speed ($N=82000$ rpm), mass flow rate ($\dot{m} = 0.27 \text{ kg/s}$), and turbine inlet temperature ($TIT = 985 \text{ K}$) to produce its own performance data set. Simultaneously, the GasTurb10 high-fidelity simulator was run under the same design point conditions to produce a corresponding set of performance data. The two sets of design point parameters were then compared to evaluate the accuracy of the MTCturb model at the design point. As presented in Table 2, discrepancies were more pronounced in the engine's hot section. Further analysis suggests that these deviations may stem from assumptions such as constant thermo-physical properties and the omission of thermal inertia effects in engine components.

For off-design steady-state validation, the operating line predicted by the physics-based dynamic model (MTCturb) was compared with results from the GasTurb10 simulation program. As shown in Figure 6, both models align at the design point but exhibit slight deviations as engine speed decreases. These discrepancies may stem from simplifications in component matching assumptions, variations in thermophysical properties, or measurement uncertainties. Table 2 presents a comparative analysis of key performance parameters, including mass flow rate and pressure ratios. The root mean square error

Table 1. Design point validation results.

Parameter	Dynamic Model	Gasturb10	Error %
Thrust (N)	87.7	90	2.56
Fuel flow rate (kg/s)	0.0043	0.0041	4.87
Specific fuel consumption (kg/h.N)	0.175	0.171	2.39
P_{01} (kPa)	101.32	101.32	0.00
T_{01} (K)	288.15	288.15	0.00
P_{02} (kPa)	331.83	331.84	3.01
T_{02} (K)	467.28	465.58	0.36
P_{03} (kPa)	328.52	328.52	0.00
T_{03} (K)	985	985	0.00
P_{04} (kPa)	127.11	132.92	4.37
T_{04} (K)	820.87	827	0.85
P_{05} (kPa)	127.11	132.92	4.37
T_{05} (K)	820.87	827	0.85

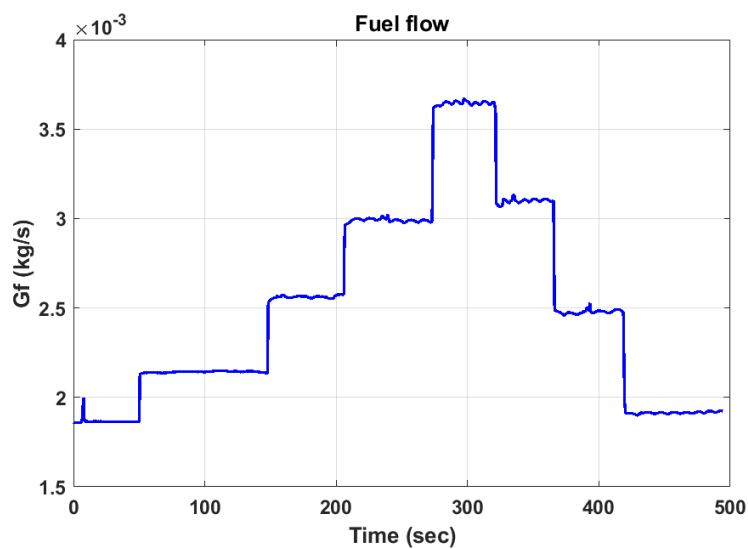
(RMSE) between the two models was calculated as 4.43% for the corrected mass flow rate and 2.39% for the compressor pressure ratio.

**Figure 6.** Off-design steady-state operating line comparison.

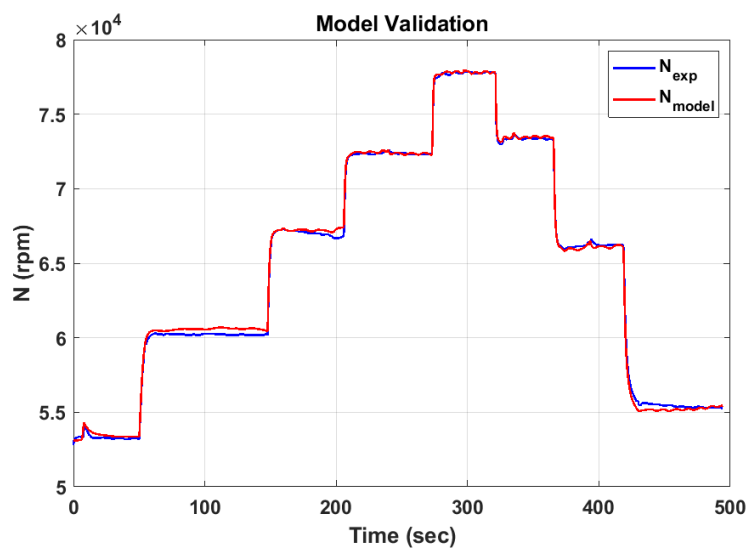
Finally, the off-design transient performance of the physics-based dynamic model (MTCTurb) was evaluated by simulating the engine's response to fuel flow variations obtained from experimental data, as shown in Figure 7a. The model's accuracy was validated by comparing its predicted shaft speed response with experimental data from engine testing under the same input variations, as illustrated in Figure 7b. The results demonstrated strong agreement, with a mean square error (MSE) of 0.116%, indicating high precision. As shown in Figure 8, the small deviation between the predicted and measured values confirms the model's reliability in capturing transient engine behavior.

Table 2. Off-design steady-state operating line data comparison.

Relative Speed	Error% in m_c^\bullet	Error % in π_C
1	0.0186	0.549
0.95	0.010	1.270
0.9	0.305	2.749
0.85	0.873	3.358
0.8	1.529	2.984
0.75	1.915	2.837
0.7	2.042	2.270
0.65	12.08	1.686



(a) Model input.



(b) Model output.

Figure 7. Physics based model validation.

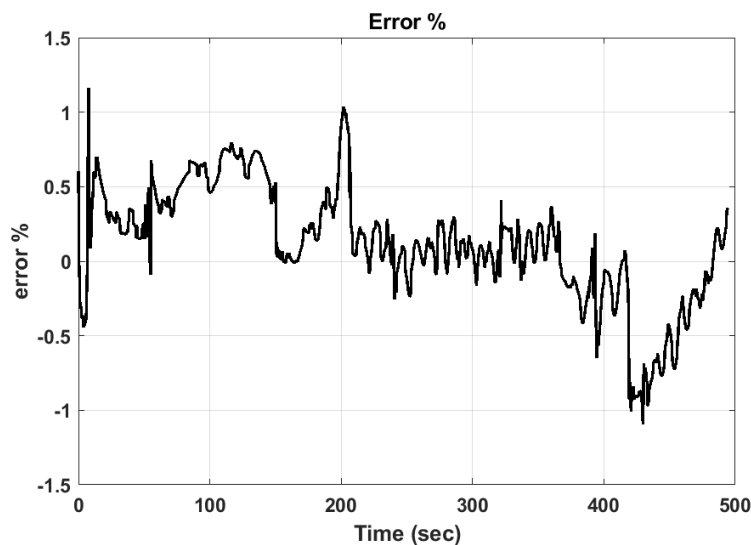


Figure 8. Physics based model validation accuracy.

5. Conclusion

This study presented a physics-based dynamic modeling approach for analyzing the steady-state and transient performance of a micro gas turbine engine (MGTE). The developed model (MTCturb) accurately predicts engine behavior under off-design conditions by incorporating component matching calculations and dynamic response analysis. Both off-design steady-state and transient-state simulations were validated against experimental data and Gasturb10 software results, demonstrating good agreement. The mean square error (MSE) of 0.116 % between the model (MTCturb) output and experimental data confirms the model's accuracy and reliability.

Despite its effectiveness, certain assumptions, such as constant thermophysical properties and neglected thermal inertia, may contribute to minor discrepancies. Future improvements could focus on enhanced heat temperature and pressure dynamic modeling. Additionally, optimizing the computational efficiency of the model could enable real-time simulations, making it a real time high-fidelity tool for control system development and performance monitoring in practical applications.

References

- [1] Ibrahim, I. M., Akhrif, O., Staniszewski, M., and Moustapha, H., 2020. "Real time modeling and hardware in the loop simulation of an aero-derivative gas turbine engine". *Proceedings of Global Power & Propulsion Society*.
- [2] Asgari, H., Chen, X., and Sainudiin, R., 2013. "Modelling and simulation of gas turbines". *International Journal of Modelling, Identification and Control*, **20**(3), pp. 253–270.
- [3] Aly, A., and Atia, I., 2012. "Neural modeling and predictive control of a small turbojet engine (sr-30)". In 10th International Energy Conversion Engineering Conference, p. 4242.
- [4] Ibrahim, I. A., Akhrif, O., Moustapha, H., and Staniszewski, M., 2020. "An ensemble of recurrent neural networks for real time performance modelling of three-spool aero-derivative gas turbine engine".
- [5] Mehrpanahi, A., Hamidavi, A., and Ghorbanifar, A., 2018. "A novel dynamic modeling of an industrial gas turbine using condition monitoring data". *Applied Thermal Engineering*, **143**, pp. 507–520.
- [6] Nguyen, T. V., 2000. "A method to identify the parametric dynamic model of a single-shaft gas turbine engine". PhD thesis, Colorado State University.
- [7] Sanghi, V., Lakshmanan, B., and Sundararajan, V., 2000. "Survey of advancements in jet-engine thermodynamic simulation". *Journal of Propulsion and Power*, **16**(5), pp. 797–807.

- [8] H.I.H. Saravanamuttoo, G.F.C. Rogers, P. S. H. C. A., 2017. *Gas Turbine Theory*, 7 ed. Pearson.
- [9] Kyprianidis, K., and Kalfas, A. I., 2008. "Dynamic performance investigations of a turbojet engine using a cross-application visual oriented platform". *The Aeronautical Journal*, **112**(1129), pp. 161–169.
- [10] Yazar, I., Yasa, T., and Kiyak, E., 2017. "Simulation-based steady-state aero-thermal model for small-scale turboprop engine". *Aircraft Engineering and Aerospace Technology*.
- [11] Gu, C.-w., Wang, H., Ji, X.-x., and Li, X.-s., 2016. "Development and application of a thermodynamic-cycle performance analysis method of a three-shaft gas turbine". *Energy*, **112**, pp. 307–321.
- [12] Zhou, Q., Yin, Z., Zhang, H., Wang, T., Sun, W., and Tan, C., 2020. "Performance analysis and optimized control strategy for a three-shaft, recuperated gas turbine with power turbine variable area nozzle". *Applied Thermal Engineering*, **164**, p. 114353.
- [13] Fawke, A., and Saravanamuttoo, H., 1971. "Digital computer methods for prediction of gas turbine dynamic response". *SAE Transactions*, pp. 1805–1813.
- [14] Thirunavukarasu, E., 2013. "Modeling and simulation study of a dynamic gas turbine system in a virtual test bed environment".
- [15] Forhad, M. M. I., and Bloomberg, M., 2015. "Drive train over-speed prediction for gas fuel based gas turbine power generation units". In *Turbo Expo: Power for Land, Sea, and Air*, Vol. 56758, American Society of Mechanical Engineers, p. V006T05A024.
- [16] Petkovic, D., Banjac, M., Milic, S., Petrovic, M. V., and Wiedermann, A., 2019. "Modelling the transient behaviour of gas turbines". In *Turbo Expo: Power for Land, Sea, and Air*, Vol. 58554, American Society of Mechanical Engineers, p. V02AT45A014.
- [17] Zhu, P., and Saravanamuttoo, H., 1992. "Simulation of an advanced twin-spool industrial gas turbine".
- [18] Tsoutsanis, E., Meskin, N., Benammar, M., and Khorasani, K., 2013. "Dynamic performance simulation of an aeroderivative gas turbine using the matlab simulink environment". In *ASME 2013 International Mechanical Engineering Congress and Exposition*, American Society of Mechanical Engineers Digital Collection.
- [19] Wang, C., 2016. "Transient performance simulation of gas turbine engine integrated with fuel and control systems".
- [20] Singh, R., Maity, A., and Nataraj, P. S., 2022. "Dynamic modeling and robust nonlinear control of a laboratory gas turbine engine". *Aerospace Science and Technology*, **126**, p. 107586.
- [21] Nott, C., Ölçmen, S. M., Karr, C. L., and Trevino, L. C., 2007. "Sr-30 turbojet engine real-time sensor health monitoring using neural networks, and bayesian belief networks". *Applied Intelligence*, **26**, pp. 251–265.
- [22] Lichtsinder, M., and Levy, Y., 2006. "Jet engine model for control and real-time simulations". *Journal of Engineering for Gas Turbines and Power*, **128**(4), pp. 745–753.
- [23] Valencia-Bravo, J. M., 2010. "On-line performance parameter estimation of sr-30 turbojet engine". PhD thesis.
- [24] Sellers, J. F., and Daniele, C. J., 1975. *DYNGEN: A program for calculating steady-state and transient performance of turbojet and turbofan engines*, Vol. 7901. National Aeronautics and Space Administration.
- [25] Gaudet, S. R., 2008. "Development of a dynamic modeling and control system design methodology for gas turbines". PhD thesis, Carleton University.
- [26] Kurzke, J., 2004. *Gasturb10 technical reference*.